Near-field Raman spectroscopy of biological nanomaterials by *in situ* laser-induced synthesis of tip-enhanced Raman spectroscopy tips

Faris Sinjab,[1] Banyat Lekprasert,[1] Richard A. J. Woolley,[1] Clive J. Roberts,[2] Saul J. B. Tendler,[2] and Ioan Notingher[1,*]

[1]*School of Physics and Astronomy, University of Nottingham, University Park, Nottingham NG7 2RD, United Kingdom*

[2]*School of Pharmacy, University of Nottingham, University Park, Nottingham NG7 2RD, United Kingdom*

**Corresponding author: ioan.notingher@nottingham.ac.uk*

Received December 19, 2011; revised April 18, 2012; accepted April 18, 2012; posted April 18, 2012 (Doc. ID 160273); published June 6, 2012

We report a new approach in tip-enhanced Raman spectroscopy (TERS) in which TERS-active tips with enhancement factors of ~10^{-5}× can be rapidly (1–3 min) produced *in situ* by laser-induced synthesis of silver nanoparticles at the tip apex. The technique minimizes the risks of tip contamination and damage during handling and provides *in situ* feedback control, which allows the prediction of the tip performance. We show that TERS tips produced by this technique enable the measurement of spatially resolved TERS spectra of self-assembled peptide nanotubes with a spatial resolution of ~20 nm.

OCIS codes: 180.4243, 300.6450, 120.4570.

Tip-enhanced Raman spectroscopy (TERS) is an emerging technique that combines the chemical sensitivity of Raman spectroscopy with the high resolution of scanning probe microscopy (SPM) [1–3]. TERS is based on the resonant interaction of light with surface plasmons in sharp metal tips, which are brought in the vicinity of the sample by the aid of an SPM, leading to a ~10^4–10^6 fold enhancement for the Raman spectrum of the sample surface (~1–5 nm top layer) [4]. Recently, TERS has been used to study biological samples, such as nucleic acids [5], proteins [6–8], viruses [9], and cells [10,11]. However, one of the main limitations of TERS is the low yield of TERS active tips and the difficulty in predicting their TERS activity and lifetime [8,12]. The most common method for fabrication of TERS tips for the analysis of biological samples relies on off-line thermal evaporation of silver/gold on an atomic force microscopy (AFM) tip. However, the intrinsic limitation of the off-line techniques is that the apex geometry cannot be controlled and the delay between fabrication and use often leads to tip contamination, oxidation, and mechanical damage. Therefore, the TERS enhancing performance of these tips is unpredictable [8,12].

We report a new method for engineering TERS tips that has the potential to overcome the limitations of the current off-line methods. We show that TERS-active tips can be fabricated *in situ* by using the laser of the TERS instrument to induce the controlled synthesis of silver nanoparticles at the tip apex. Such tips can be used immediately to record TERS spectra of a sample; therefore the risks of contamination, mechanical and electrostatic damage during handling are minimized.

The TERS instrument was based on an AFM mounted on an inverted optical microscope to which a 532 nm laser and spectrometer were coupled [13]. AFM topography and TERS measurements were carried out by sample scanning with the tip fixed in position corresponding to the maximum intensity of the backscattered laser light. TERS tips were grown by mounting the AFM tips (AC240TS, Asylum AFM and OLTESPA, Bruker) on the TERS instrument and then dipping the tips in a solution of 0.4 mM $AgNO_3$ mixed with 0.4 mM sodium citrate dibasic (Sigma-Aldrich) in deionized water and then illuminating with the 532 nm laser (power levels 1–5 mW) with the aid of a 20× microscope objective (Fig. 1).

Recent studies using light emitting diodes and lasers have showed that silver nanoparticles with well defined geometries can be synthesized in aqueous solutions by varying the excitation wavelength and polarization [14,15]. The energy dispersive X-ray (EDX) (silver La1 line) and transmission electron microscopy (TEM) images of typical TERS tips produced by *in situ* laser-induced synthesis [Fig. 2(a)] show that nanoparticles with different geometries can also be grown on the apex of the tips depending on the laser power and surface properties of the tips. If silicon AFM tips were used without any pre-treatment, only a low coverage of the AFM tip apex with nanoparticles was observed and the nanoparticles were predominantly spherical with diameters in the range 20–70 nm. Precoating the tips with 3-aminotriethoxysilane (APTES) (for 24 h) to increase the affinity of the nanoparticles to bind the tip led to a high coverage of the tip with Ag nanoparticles, for which the geometry depended on the power of the laser used. At 1 mW laser power, the apex of the tips had a good coverage with Ag nanospheres of ~40 nm diameter. At 5 mW laser power, a much greater abundance of Ag on the tip apex was observed in the form of nanocrystalline structures or nanorods, approximately 100–220 nm in length and 40–60 nm in diameter.

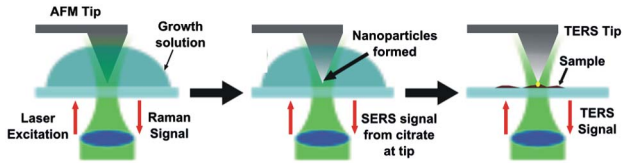

Fig. 1. (Color online) Schematic description of the *in situ* method for fabrication of TERS-active tips.

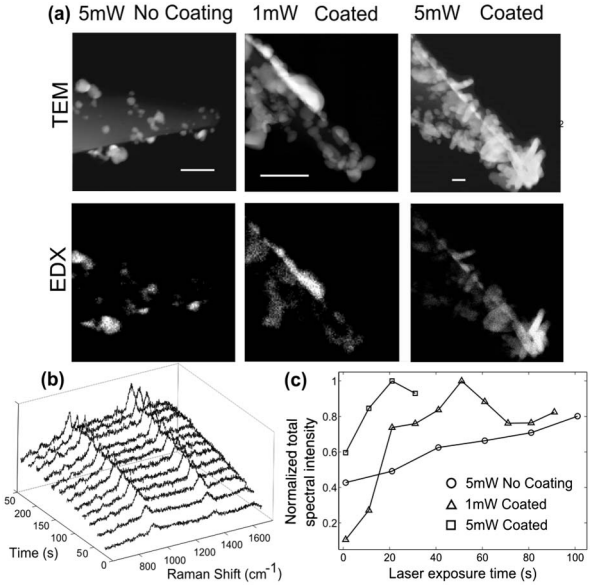

Fig. 2. (a) TEM and EDX images of typical TERS tips fabricated by the laser-induced synthesis (coating: APTES, scale bar 200 nm), (b) time-lapse SERS spectra of citrate during the growth of a tip, (c) intensity of the SERS during the tip growth for the three conditions.

The geometry of the nanoparticles grown on the AFM tips is the result of a combined effect between availability of Ag+ ions and the nanoparticle affinity to the tip. Initially, the laser induces the synthesis of Ag nanoparticles in the immediate vicinity of the tip apex (maximum electric field associated to the laser) where concentration of Ag+ ions is the highest. As the nanoparticles grow, the laser induces surface plasmon excitations in the nanoparticles, which increases further the electric field and the availability of Ag+ ions in the ~5 nm region around the nanoparticles [15]. Compared to nanoparticles synthesized in solution that are free to rotate [15], the orientation of the nanoparticles attached to the tip relative to the laser polarization will be restricted, and therefore a predominantly unidimensional growth along the laser polarization directions occurs, especially when higher laser power (5 mW) was used. This self-driven growth stops when the frequency of the longitudinal surface plasmon resonances corresponds to the frequency of the laser photons [15]. Thus, future optimization of laser wavelength and polarization (in a vertical direction) may provide a higher degree of control over the growth direction of the nanoparticles and increase their TERS activity.

During the tip growth, the Ag nanoparticles attached to the tip apex also enable the measurement of time-lapse surface enhanced Raman spectroscopy (SERS) spectra of the precursor citrate solution. Increasing bands at 940 and 1380 cm^{-1}, corresponding to the carbon-carbon ν(C-COO) and carboxylic symmetric stretching ν(-COO^-) vibrations of citrate, can be observed in Fig. 2(b). This SERS signal provides an *in situ* feedback mechanism that can be used to monitor the TERS activity of the tip during its fabrication. Figure 2(c) shows an increased growth rate of the nanoparticles due to the APTES layer with a much greater total SERS signal per unit time, predicting that the TERS activity of these tips is higher. The intensity of the SERS signal reaches a plateau after ~1–3 min [Fig. 2(c)], at which point the precursor solution can be removed and the sample of interest can be located on the instrument for TERS analysis.

As the TERS enhancement of the tips produced without APTES precoating was lower, their TERS enhancement was evaluated by measuring TERS spectra (tapping mode) of a p-aminothiophenol (pATP) monolayer adsorbed on 20 nm silver thick films (Fig. 3). The enhancement was calculated using methods described previously [16] and was estimated to be ~100×, which is at the lower end of the enhancement levels reported by other studies using Ag coated tips by thermal evaporation and similar experimental conditions [16]. The rapid decrease in the intensity of the Raman bands when the tip-distance is increased from 10 to 21 nm (the mean tip-sample distance represents the calibrated tip oscillation amplitude) is attributed to the fast decrease of the near-field intensity at the tip apex. As the tip is retracted in the far-field (1–10 μm), the intensity of the Raman bands decreases slowly as the tip apex gets out of focus and the back-scattering of the Raman signal decreases.

When the same laser power of ~5 mW was used with tips that were precoated with APTES, the TERS tips produced large fluctuations in the TERS spectra; therefore they were not suitable for TERS measurements.

TERS tips with high and consistent enhancements were obtained when tips precoated with APTES were illuminated at 1 mW laser power. TERS spectra of individual diphenylalanine nanotubes measured with such tips are shown in Fig. 4 (details on the methods for fabrication of the nanotubes can be found in [17]). The diphenylalanine peptide (L-Phe-L-Phe; FF) is the core recognition motif for self-assembly of the β-amyloid peptide; therefore the study of these materials is relevant for understanding neurodegenerative diseases [18]. Self-assembled diphenylalanine-based peptides have also led recently to an increased research interest in using these molecules as building blocks for fabrication of biocompatible nanostructures for various applications [19]. The AFM image allowed the measurement of the nanotube diameters (nanotube height) as 80 nm, while the profile of the 1056 cm^{-1} band in the TERS spectra across the nanotube shows a FWHM of ~100 nm, which corresponds to a spatial resolution of ~20 nm.

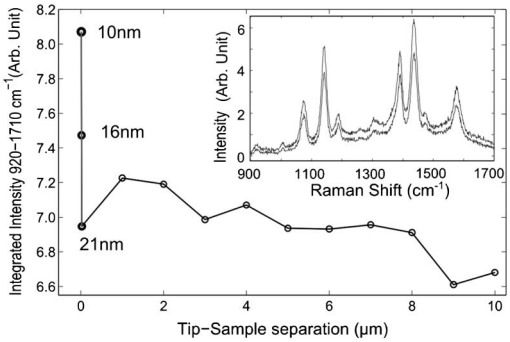

Fig. 3. TERS of pATP monolayer using TERS tips formed at 5 mW laser power and no precoating: effect of tip-sample distance on TERS signal intensity. Inset: TERS spectra at 10 nm tip-sample separation (top) compared to the spectrum with tip retracted (bottom). For TERS: 100 μW laser power, 20 s acquisition time.

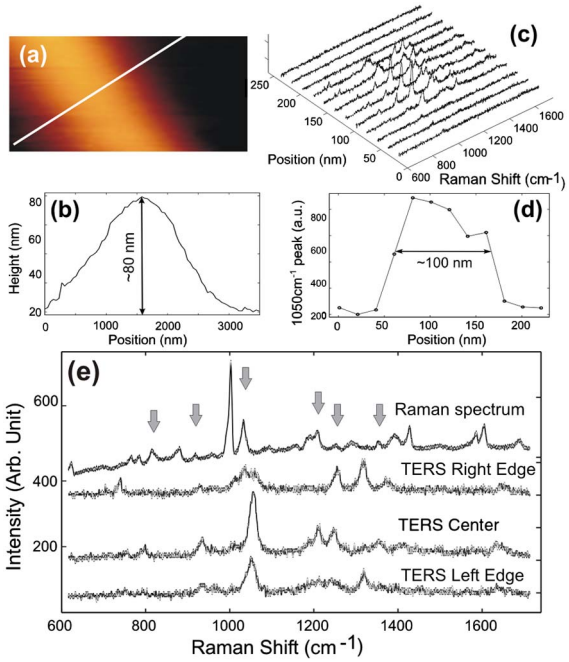

Fig. 4. (Color online) TERS of an FF nanotube using a tip fabricated by APTES precoating and 1 mW laser power: (a), (b) topography and height profile along the white line, (c) TERS spectra across the nanotube, (d) line profile corresponding to the 1056 cm^{-1} TERS band, (e) comparison between the Raman spectrum of a 2.5 μm diameter FF tube and the spatially resolved TERS of the nanotube in (a). For TERS: 100 μW laser power, 50 s acquisition time.

Although most of the bands present in the TERS spectra of the FF nanotubes can also be found in the spontaneous Raman spectra (~2.5 μm diameter tube), the relative intensity of the bands is different [Fig. 4(e)]. Several bands in the TERS spectra can be assigned to the aromatic groups at 1056 cm^{-1} (in-plane CH bending) and 1216 cm^{-1} (CH bending with ring stretching), and they are found at 1031 and 1198 cm^{-1} in the Raman spectra of FF nanotubes [19]. The strong 1003 cm^{-1} Raman band (symmetric breathing of phenyl) is missing, which is in agreement with previous TERS spectra of phenylalanine amino acids, insulin fibers, and virus capsids [6–9]. The TERS spectra also show bands at 934, 1247, and 1319 cm^{-1}, assigned to the C-COO- stretching, Amide III and CH_2 deformations [6–9].

Importantly, Fig. 4(c) shows that he 1056 cm^{-1} band associated to the phenyl groups has a maximum intensity at the center of the nanotube and decreases towards the edges. In contrast, the band at 1319 cm^{-1} is absent at the center and has a maximum intensity at the edges of the nanotube. As only the vertical component of the laser electric field leads to the excitation of surface plasmons at the tip apex, only vibrations with polarizability components in this direction will be enhanced in TERS [4,6]. Therefore the differences between the TERS spectra measured at the center and edges of the FF nanotube may be due to the different orientation of the molecules at the nanotube surface relative to the vertical direction of the TERS tip [8]. However, effects due to nonuniformity of the TERS tips may also contribute to the spectral differences. Based on the intensity of the Raman spectra measured for larger tubes (diameter ~2 μm) and TERS on smaller nanotubes (diameter <100 nm), and accounting for the sampling volumes [16], the TERS enhancement was estimated to ~10^5× (sampling depth for TERS ~5 nm, based on [4] and considering a refractive index of 1.4 for the FF nanotubes).

In summary, we have presented a novel method for rapid and controlled fabrication of TERS active tips that has the potential to overcome the main limitations of the conventional off-line methods. While the removal of the precursor solution and sample mounting involves a certain level of risks of contamination and damage, these risks are considerably reduced compared to the off-line methods. Future studies are required to optimize the fabrication technique, for example by controlling the polarization, wavelength of the laser, and other tip precoatings, to produce TERS tips with well defined apex geometries.

We thank Drs. M. Fay and C. Parmenter (Nottingham Nanotechnology and Nanoscience Centre) for the characterization of the TERS tips by electron microscopy.

References

1. R. M. Stöckle, Y. Doug Suh, V. Deckert, and R. Zenobi, Chem. Phys. Lett. **318**, 131 (2000).
2. A. Hartschuh, E. J. Sánchez, X. S. Xie, and L. Novotny, Phys. Rev. Lett. **90**, 095503 (2003).
3. B. Pettinger, B. Ren, G. Picardi, R. Schuster, and G. Ertl, Phys. Rev. Lett. **92**, 096101 (2004).
4. I. Notingher and A. Elfick, J. Phys. Chem. B **109**, 15699 (2005).
5. E. Bailo and V. Deckert, Angew. Chem. Int. E. **47**, 1658 (2008).
6. T. Deckert-Gaudig, E. Rauls, and V. Deckert, J. Phys. Chem. C **114**, 7412 (2010).
7. B.-S. Yeo, S. Madler, T. Schmid, W. Zhang, and R. Zenobi, J. Phys. Chem. C **112**, 4867 (2008).
8. T. Deckert-Gaudig and V. Deckert, Phys. Chem. Chem. Phys. **12**, 12040 (2010).
9. D. Cialla, T. Deckert-Gaudig, C. Budich, M. Laue, R. Moller, D. Naumann, V. Deckert, and J. Popp, J. Raman Spectrosc. **40**, 240 (2009).
10. M. Richter, M. Hedegaard, T. Deckert-Gaudig, P. Lampen, and Volker Deckert, Small **7**, 209 (2011).
11. B. R. Wood, E. Bailo, M. A. Khiavi, L. Tilley, S. Deed, T. Deckert-Gaudig, D. McNaughton, and V. Deckert, Nano Lett. **11**, 1868 (2011).
12. B.-S. Yeo, J. Stadler, T. Schmid, R. Zenobi, and W. Zhang, Chem. Phys. Lett. **472**, 1 (2009).
13. C. S. Sweetenham, M. Larraona-Puy, and I. Notingher, Appl. Spectrosc. **65**, 1387 (2011).
14. K. G. Stamplecoskie and J. C. Scaiano, J. Am. Chem. Soc. **132**, 1825 (2010).
15. M. Maillard, P. R. Huang, and L. Brus, Nano Lett. **3**, 1611 (2003).
16. D. Roy, J. Wang, and C. Williams, J. Appl. Phys. **105**, 013530 (2009).
17. B. Lekprasert, V. Sedman, C. J. Roberts, S. J. Tendler, and I. Notingher, Opt. Lett. **35**, 4193 (2010).
18. A. T. Petkova, R. D. Leapman, Z. Guo, W.-M. Yau, M. P. Mattson, and R. Tycko, Science **307**, 262 (2005).
19. X. Yan, P. Zhu, and J. Li, Chem. Soc. Rev. **39**, 1877 (2010).